Phenomenological and Microscopic Analysis of Elastic Scattering Reactions of ^{20}Ne by ^{12}C, ^{16}O, ^{28}Si, ^{58}Ni

MURAT AYGÜN

Department of Physics, Bitlis Eren University, Bitlis 13000, Turkey

Abstract

In this study, the elastic scattering angular distributions of ^{20}Ne from ^{12}C, ^{16}O, ^{28}Si and ^{58}Ni target nuclei have been investigated at various incident energies. For this, both the phenomenological model and the double folding model have been used. In the phenomenological calculations, the real and imaginary potentials have been evaluated in Woods-Saxon type. In the double folding calculations, the imaginary part has been assumed as Woods-Saxon potential while the real part has been obtained by using the folding model. The theoretical results have been compared with the literature as well as the experimental data. It has been observed that our results have been in agreement with the experimental data. Also, the cross-sections of the investigated system and models have been given.

Keywords: Optical model, double folding model, elastic scattering.

1. Introduction

The optical model (OM) is one of the most effective methods in explaining the elastic scattering cross section of projectile by target nucleus. To determine the optical potential of system investigated, the phenomenological model (PM) and the double folding model (DFM) (SATCHLER and Love, 1979) are often applied. Thus, the optical potential is obtained by searching of the potential parameters of model assumed. It is well-known that the OM parameters are extensively used in the calculations of elastic scattering, coupled-channels, transfer reactions. While the OM parameters for multiple systems are defined, one of the most preferred ways is to find the parameters for the same potential geometry of the systems.

Received: 22.05.2017
Revised: 07.08.2017
Accepted:28.09.2017
Corresponding author: Murat Aygun, PhD
Department of Physics, Bitlis Eren University, Bitlis 13000, Turkey
E-mail: murata.25@gmail.com
Cite this article as: M. Aygun, Phenomenological and Microscopic Analysis of Elastic Scattering Reactions of ^{20}Ne by ^{12}C, ^{16}O, ^{28}Si, ^{58}Ni, Eastern Anatolian Journal of Science, Vol. 3, Issue 2, 8-15, 2017.

Due to the fact that the interactions of projectile with different target nuclei have different potentials, it is difficult to work on the same potential geometry. Consequently, establishing potential parameters has been both difficult and important in the examination of nuclear reactions. In literature, the theoretical studies performed with this goal can be found at Ref. (AYGUN, 2014; AYGUN et al. 2010).

In the last few decades, various experimental and theoretical studies have been carried out on ^{20}Ne nucleus (PIASECKI et al. 2012; PARKER et al. 1987; TILLEY, 1998; SINGH et al. 2008; HEIL et al. 2014). Some of these works have been on the elastic scattering of ^{20}Ne nucleus with different target nuclei over several incident energies. Doubre et al. (1978) measured the elastic scattering of ^{20}Ne+^{12}C system at E_{Lab}=65.86 MeV and analyzed the experimental data by means of the OM. Bohlen et al. (1993) reported the elastic scattering, inelastic scattering and one neutron transfer channels of ^{20}Ne+^{12}C system at E_{Lab}=390 MeV. They performed the OM and DFM analysis to explain the experimental data of this system which presents a strong absorption. Miao et al. (1996) obtained the elastic scattering angular distributions of ^{20}Ne+^{16}O system at different energies. To explain the experimental data, they presented the theoretical results acquired by using the OM. The elastic scattering data of ^{20}Ne on ^{28}Si have been reported by (SOUKERAS, 2013; SGOUROS, 2013; SGOUROS et al. 2013). They analyzed the experimental data with the distorted wave born approximation (DWBA), the OM and the coupled reaction channels (CRC). Bohlen et al. [1985] measured the elastic scattering of ^{20}Ne+^{58}Ni system at E_{Lab}=291 and 392 MeV and investigated the experimental data within the OM. However, as far as we know, if one seeks the optical potential parameters for the same potential geometry of these systems, one can not find them in literature. We aim to obtain the potential parameters of ^{20}Ne+^{12}C, ^{20}Ne+^{16}O, ^{20}Ne+^{28}Si and ^{20}Ne+^{58}Ni reactions at different incident energies with the same potential geometry. Thus, these potential parameters will be able to use in the calculations of both new energies of these systems with ^{20}Ne and different nucleus reactions with ^{20}Ne. Additionally, these parameters will be important in the experimental analysis of

coupled-channels, transfer reactions, α-folding model of ^{20}Ne.

In this study, we examine ^{20}Ne-nucleus reactions with a phenomenological way within the framework of OM. Then, we analyze all the reactions by using the DFM within the microscopic model. We show the optical potential parameters of the PM and DFM. Finally, we compare the PM and DFM results with previous theoretical and experimental studies.

2. Theoretical Formalism

In the present work, the elastic scattering data of ^{20}Ne is investigated using PM and DFM at various incident energies. For this, different target nuclei are used from ^{12}C to ^{58}Ni. In this concept, the total effective potential, $V_{total}(r)$, is given by,

$$V_{total}(r) = V_{nuclear}(r) + V_{Coulomb}(r) \quad (1)$$

where $V_{nuclear}(r)$ is nuclear potential and $V_{Coulomb}(r)$ is Coulomb potential. The Coulomb potential is taken as (SATCHLER, 1983),

$$V_{Coulomb}(r) = \begin{cases} \frac{1}{4\pi\varepsilon_0}\frac{Z_P Z_T e^2}{r}, & r \geq R_C \\ \frac{1}{4\pi\varepsilon_0}\frac{Z_P Z_T e^2}{2R_C}\left(3 - \frac{r^2}{R_C^2}\right), & r < R_C \end{cases} \quad (2)$$

$$R_c = 1.25\left(A_P^{1/3} + A_T^{1/3}\right) \quad (3)$$

where Z_P and Z_T, respectively, are the charges of the projectile and target nuclei, R_c is the Coulomb Radius, A_P and A_T are the projectile and target masses, respectively.

2.1 Phenomenological Model Analysis

In general sense, the PM assumes Woods-Saxon (WS) or Woods-Saxon squared (WS^2) type potentials for the real and imaginary parts of the optical potential. In this sense, the nuclear potential is given by,

$$V_{nuclear}(r) = -\frac{V_0}{1+\exp\left(\frac{r-r_v\left(A_P^{1/3}+A_T^{1/3}\right)}{a_v}\right)} - \frac{iW_0}{1+\exp\left(\frac{r-r_w\left(A_P^{1/3}+A_T^{1/3}\right)}{a_w}\right)} \quad (4)$$

The potential parameters are obtained by searching of the values which fit the experimental data. This procedure is described below.

2.2 Double Folding Model Analysis

The DFM gives the real part of the optical potential over the densities of projectile and target nuclei by using an nucleon-nucleon interaction potential (v_{NN}). For this purpose, the double folding potential is written as,

$$V_{\mathrm{DF}}(\boldsymbol{r}) = \int d\boldsymbol{r_1} \int d\boldsymbol{r_2} \rho_P(\boldsymbol{r_1}) \rho_T(\boldsymbol{r_2})\, v_{NN}(r_{12}) \quad (5)$$

where $\rho_P(\boldsymbol{r_1})$ and $\rho_T(\boldsymbol{r_2})$ are the nuclear matter densities of projectile and target nuclei, respectively. In the present work, the density distributions of both projectile and target nuclei except for ^{12}C have been taken from RIPL-3 (RIPL-3). ^{12}C density is written as,

$$\rho_{12_C}(r) = \rho_0(1 + wr^2)\exp(-\beta r^2) \quad (6)$$

where ρ_0 = 0.1644 fm^{-3}, w = 0.4988 fm^{-2}, and β = 0.3741 fm^{-2} (FARID and HASSANIAN, 2000; KARAKOC and BOZTOSUN, 2006). In Fig. 1, the proton and neutron density distributions used for ^{20}Ne nucleus are displayed. In folding model calculations, we have chosen the M3Y (Michigan 3 Yukawa) nucleon-nucleon realistic interaction given by,

$$v_{NN}(r) = 7999\frac{\exp(-4r)}{4r} - 2134\frac{\exp(-2.5r)}{2.5r} - 276[1 - 0.005E_{\mathrm{Lab}}/A_P]\delta(r) \quad (7)$$

Finally, the imaginary part of optical potential is assumed WS type as in the form

$$W(r) = -\frac{W_0}{1+\exp\left(\frac{r-r_w\left(A_P^{1/3}+A_T^{1/3}\right)}{a_w}\right)} \quad (8)$$

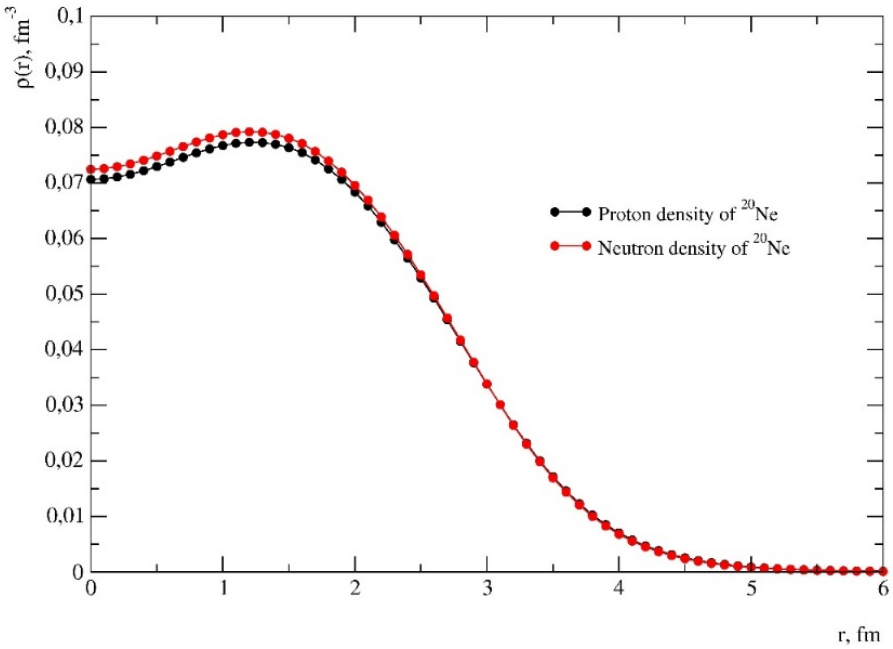

Figure 1. The proton and neutron density distributions of ^{20}Ne nucleus.

2.3 Fitting Procedure

In this section, we introduce fitting procedure used in PM and DFM calculations. While the values of the real and imaginary potentials to be used in the phenomenological analysis have been defined, we have started from the potential values reported in the literature (DOUBRE et al. 1978; BOHLEN et al. 1993; MIAO et al. 1996; SOUKERAS, 2013; BOHLEN et al. 1985). Then, we have performed compliance tests between the experimental data and the theoretical results of all the systems investigated in our work. In order to obtain the OM parameters at the same potential geometries of reactions, we have searched the values of r_v=r_w and a_v=a_w. After the test calculations performed to obtain results compatible with the experimental data, we have taken as 0.913 fm the values of r_v=r_w. Then, for this value of r_v and r_w, we have examined the values of a_v and a_w which give good agreement results with the data. We have found 0.78 fm for a_v = a_w. We have eventually searched V_0 and W_0 values at the values determined of r_v=r_w and a_v=a_w. We have given the OM parameters obtained for all the reactions by means of the PM in Table I.

In DFM calculations, the values W_0, r_w and a_w of imaginary potential have been obtained as described above. According to this, firstly, the value r_w in steps of 0.1 fm at each incident energy has been investigated and kept constant at 1.32 fm. Then, the value a_w of imaginary potential has been varied in steps of 0.1 and 0.01 fm for fixed radius and has been taken as 0.55 fm. Finally, the fitting procedure has been completed by adjusting only the depth of imaginary potential. The optical potential parameters of all the reactions within the framework of DFM have been shown in Table II.

The code FRESCO (THOMPSON, 1988) has been used in the theoretical calculations.

3. Results and Discussion

We have analyzed the elastic scattering data of ^{20}Ne+^{12}C reaction at incident energies E_{Lab}=65.86 and 390 MeV. For this, we have used the PM and the DFM within the framework of OM. The values of potential parameters for each model are given in Tables I and II. Also, all theoretical results with PM and DFM are compared with the experimental data as shown in Fig. 2. Although it is difficult to define the potential parameters because of both the oscillatory structure of experimental data and the same potential geometry of the systems, the results are in agreement with the experimental data for the PM and the DFM at 65.86 MeV. At 390 MeV, we have obtained very good results with the data at all angles for the PM, whereas the DFM results are not as good as the PM results. We have found a deep imaginary potential which means a strong absorption in the analysis of PM. This result is similar to the result of Ref. (BOHLEN et al. 1993). In folding model calculations, we have also investigated the change of normalization constant (N_R) and have given N_R values for examined system and energy in Table II.

Table I. The OM parameters used in PM analysis of ^{20}Ne scattered from ^{12}C, ^{16}O, ^{28}Si and ^{58}Ni target nuclei.

System	E_{Lab}	V	r_v	a_v	W	r_w	a_w	σ
	MeV	*MeV*	*fm*	*fm*	*MeV*	*fm*	*fm*	*mb*
^{20}Ne+^{12}C	65.86	24.3	0.913	0.78	5.70	0.913	0.78	736.6
	390	75.0	0.913	0.78	88.0	0.913	0.78	1742.8
^{20}Ne+^{16}O	45	49.4	0.913	0.78	2.42	0.913	0.78	475.2
	53.75	84.0	0.913	0.78	5.10	0.913	0.78	808.6
^{20}Ne+^{28}Si	42.5	148	0.913	0.78	26.0	0.913	0.78	393.8
	52.3	109	0.913	0.78	27.0	0.913	0.78	704.4
^{20}Ne+^{58}Ni	291	128	0.913	0.78	36.0	0.913	0.78	1911.0
	392	142	0.913	0.78	71.0	0.913	0.78	2214.4

Table II. The OM parameters used in DFM analysis of ^{20}Ne scattered from ^{12}C, ^{16}O, ^{28}Si and ^{58}Ni target nuclei.

System	E_{Lab}	N_R	W	r_w	a_w	σ
	MeV		*MeV*	*fm*	*fm*	*mb*
^{20}Ne+^{12}C	65.86	0.407	4.60	1.32	0.55	1071.5
	390	0.749	22.0	1.32	0.55	1826.1
^{20}Ne+^{16}O	45	0.60	4.10	1.32	0.55	754.2
	53.75	0.80	5.95	1.32	0.55	1034.5
^{20}Ne+^{28}Si	42.5	1.00	8.0	1.32	0.55	464.5
	52.3	1.00	22.0	1.32	0.55	991.4
^{20}Ne+^{58}Ni	291	0.78	9.30	1.32	0.55	2377.8
	392	0.93	10.5	1.32	0.55	2499.5

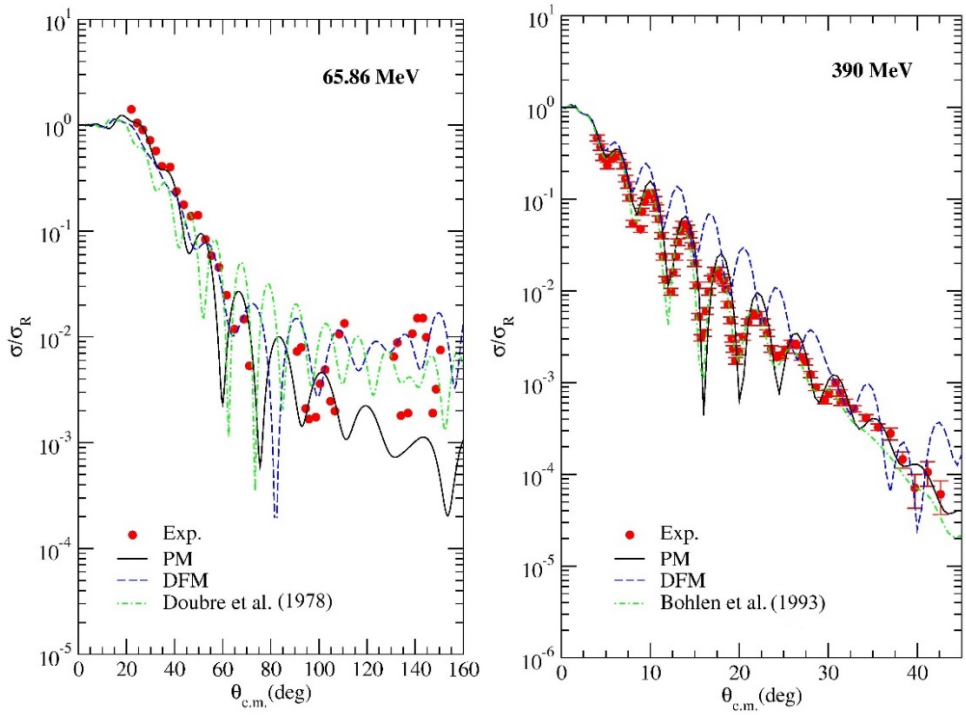

Figure 2. The elastic scattering angular distributions for ^{20}Ne+^{12}C at E_{Lab}=65.86 and 390 MeV. The solid lines show PM results; dashed lines show DFM results and dot-dashed lines show the results obtained by Doubre et al. (1978) and Bohlen et al. (1993). The circles show the experimental data, which have been taken from (DOUBRE et al. 1978; BOHLEN et al. 1993).

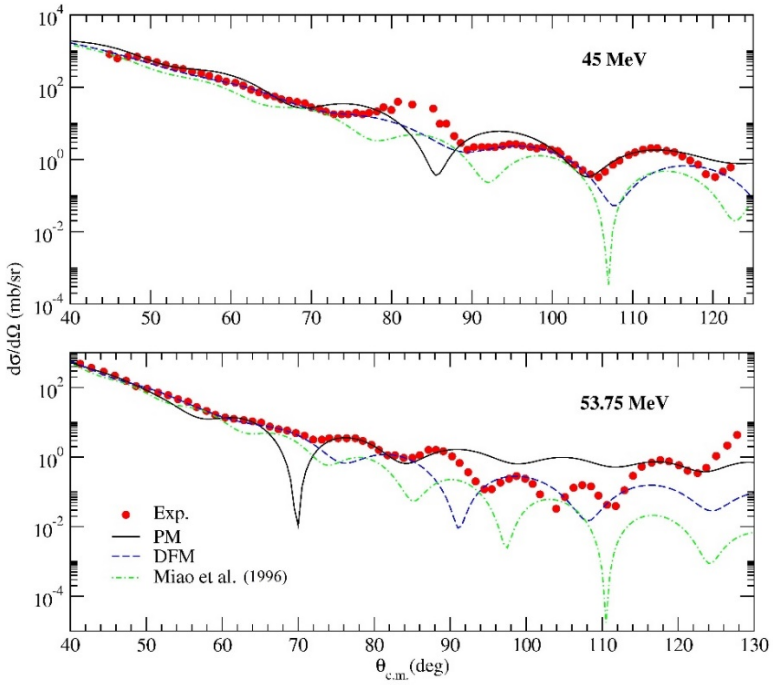

Figure 3. The elastic scattering angular distributions for ^{20}Ne+^{16}O at E_{Lab}=45 and 53.75 MeV. The solid lines show PM results; dashed lines show DFM results and dot-dashed lines show the results obtained by Miao et al. (1996). The circles show the experimental data, which have been taken from (MIAO et al. 1996).

^{20}Ne+^{16}O which has the elastic scattering data at E_{Lab}=45 and 53.75 MeV is another system investigated in our study. ^{20}Ne+^{16}O has an oscillation data for these energies. We have given the values of potential parameters obtained from the theoretical calculations of each model in Tables I and II. In Fig. 3, the theoretical results of the PM and the DFM have been exhibited in comparison with the results of the literature (MIAO et al. 1996). We have observed that the PM results are in good agreement with data and are also better than the results of Ref. (MIAO et al. 1996). In addition to this, the results of DFM are better than the the results of Ref. (MIAO et al. 1996).

In our work, we have also studied the elastic scattering of ^{20}Ne by ^{28}Si at E_{Lab}=42.5 and 52.3 MeV. Theoretical results obtained for the values shown in Tables I and II have given a satisfactory description for the experimental data, which are plotted in Fig. 4. Especially, this case is very clear at 42.5 MeV. The DFM results are in very good agreement with the data. A deep imaginary potential has been used in the calculations of PM (at all energies) and DFM (especially at 52.3 MeV) in order to obtain the general slope of the experimental data.

In final analysis, we have investigated the elastic scattering angular distribution of ^{20}Ne+^{58}Ni system at E_{Lab}=291 and 392 MeV. In Fig. 5, we have exhibited all theoretical results as comparative with the previous study (BOHLEN et al. 1985) as well as the experimental data. The consistence between PM and DFM according to the experimental data is quite good. Then, we have compared our results with the results of the literature and have noticed that both PM and DFM results are good as that of the results of Ref. (BOHLEN et al. 1985).

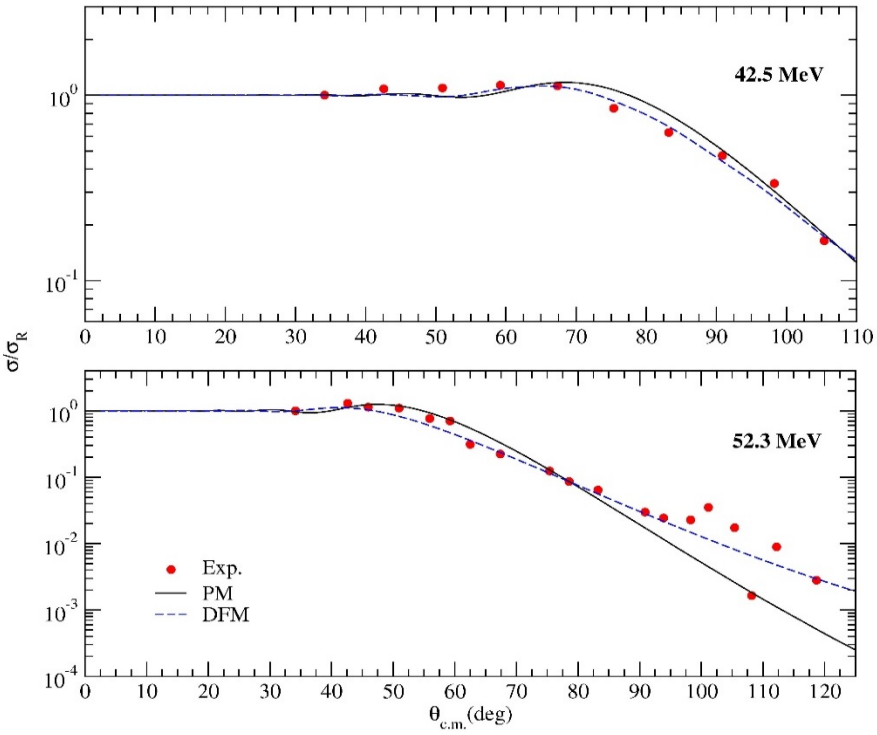

Figure 4. The elastic scattering angular distributions for ^{20}Ne+^{28}Si at E_{Lab}=42.5 and 52.3 MeV. The solid lines show PM results; dashed lines show DFM results. The circles show the experimental data, which have been taken from (SOUKERAS, 2013).

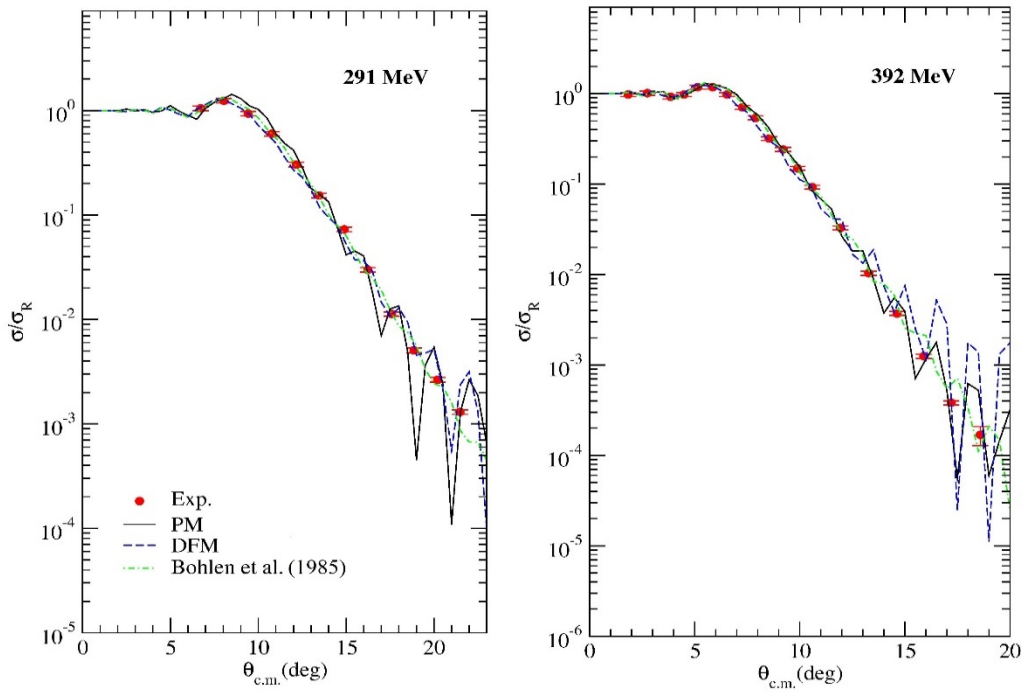

Figure 5. The elastic scattering angular distributions for ^{20}Ne+^{58}Ni at E_{Lab}=291 and 392 MeV. The solid lines show PM results; dashed lines show DFM results and dot-dashed lines show the results obtained by Bohlen et al (1985). The circles show the experimental data, which have been taken from (BOHLEN et al. 1985).

In Tables I and II, we have shown the cross-section (σ) values for all the systems investigated.
We have observed that the theoretical cross-sections of all interactions from ^{12}C to ^{58}Ni present similar behaviors with increasing of the energy. As known from previous study (AYGUN, 2012), it can be said that similar cross-sections obtained for different OM calculations such as the PM and the DFM denote good fits of the elastic scattering angular distributions.

4. Conclusions

In the present work, the elastic scattering angular distributions of ^{20}Ne on ^{12}C, ^{16}O, ^{28}Si and ^{58}Ni target nuclei have been examined. In this context, both the PM and the DFM analysis have been performed in order to explain the experimental data. The theoretical results have been compared with the results of previous studies and the experimental data. It has been noticed that our results are in agreement both with the each other and the data. The potential parameters for both investigated systems and energies by using these methods have been determined and given in tables. It can be said that the application of potential parameters obtained for ^{20}Ne interactions using the PM and the DFM based on the OM will be reliable and practical in the calculations of elastic scattering, coupled-channels, transfer reactions, α-folding model etc., of unknown reaction and energies. Moreover, the cross-sections of all the reactions have been provided. Similar behaviors of cross-sections obtained by using different OM approaches such as the PM and the DFM can be attributed to good fits of the elastic scattering angular distributions.

References

SATCHLER, G.R. and LOVE, W.G., (1979), *Folding model potentials from realistic interactions for heavy-ion scattering*, Physics Report, 55, 3.

AYGUN, M., (2014), *A microscopic analysis of elastic scattering of ^{8}Li nucleus on different target nuclei*, Acta Phys. Pol. B, 45, 9.

AYGUN, M., KUCUK, Y., BOZTOSUN, I. and IBRAHEEM, A.A., (2010), *Microscopic few-body and gaussian-shaped density distributions for the analysis of the ^{6}He exotic nucleus with different target nuclei*, Nuclear Physics A, 848, 245-259.

PIASECKI, E., et al., (2012), *Weak channels in backscattering of ^{20}Ne on ^{nat}Ni, ^{118}Sn, and ^{208}Pb*, Physical Review C, 85, 054604.

PARKER, D.J., HOGAN, J.J. and ASHER, J., (1987), *Complete and incomplete fusion in ^{20}Ne + ^{58}Nb reactions*, Physical Review C, 35, 1.

TILLEY, D.R., CHEVES, C.M., KELLEY, J.H., RAMAN, S. and WELLER, H.R., (1998), *Energy levels of light nuclei A = 20*, Nuclear Physics A, 636, 249-364.

SINGH, D., ALI R., AFZAL ANSARI, M., RASHID, M.H., GUIN, R. and DAS, S.K., (2009), *Reaction mechanisms in the system ^{20}Ne + ^{165}Ho: Measurement and analysis of forward recoil range distributions*, Physical Review C, 79, 054601.

HEIL, M., et al., (2014), *Stellar neutron capture cross sections of ^{20,21,22}Ne*, Physical Review C, 90, 045804.

DOUBRE, H., ROYNETTE, J.C., PLAGNOL, E., LOİSEAUX, J.M., MARTİN, P. and DE SAINTIGNON, P., (1978), *Experimental study of the ^{20}Ne+ ^{12}C system*, Physical Review C, 17, 131.

BOHLEN, H.G., et al., (1993), *Refractive scattering and reactions, comparison of two systems:^{16}O+^{16}O and ^{20}Ne+^{12}C*, Zeitschrift für Physik A Hadrons and Nuclei, 346, 189-200.

MIAO, Y., ZURMÜHLE R.W., BARROW, S.P., WIMER, N.G., MURGATROYD, J.T., LEE, C. and LIU, Z., (1996), *Resonant structures in the ^{20}Ne+^{16}O system*, Physical Review C, 53, 2.

SOUKERAS, V., (2013), *Elastic scattering for the system ^{20}Ne+^{28}Si at near barrier energies*, University of Ioannina, MSc Dissertation.

SGOUROS, O., (2013), *Transfer reactions for the system ^{20}Ne+^{28}Si at near barrier energies*, Master Thesis, University of Ioannina.

SGOUROS, O., et al., (2013), *Backward angle structure in the ^{20}Ne+^{28}Si quasielastic scattering*, International Journal of Modern Physics Letters E, 22, 10.

BOHLEN, H.G., OSSENBRINK, H., LETTAU, H. and OERTZEN, W.Y., (1985), *Inelastic scattering of ^{20}Ne and ^{12}C on ^{58}Ni and the three-body continuum*, Zeitschrift für Physik A Hadrons and Nuclei, 320, 237-251.

SATCHLER, G.R., (1983), *Direct Nuclear Reactions* (*Oxford University Press, Oxford*). Reference Input Parameter Library (RIPL-3), http://www-nds.iaea.org/RIPL-3.

EL-AZAB FARID, M. and HASSANIAN, M.A., (2000), *Density-independent folding analysis of the ^{6,7}Li elastic scattering at intermediate energies*, Nuclear Physics A, 678, 39.

KARAKOC, M. and BOZTOSUN, I., (2006), *α−α double folding cluster potential description of the ^{12}C+^{24}Mg system*, Physical Review C, 73, 047601.

THOMPSON, I.J., (1988), *Coupled reaction channels calculations in nuclear-physics*, Computer Physics Reports, 7, 167.

AYGUN, M., (2012), *Double-folding analysis of the ^{6}Li + ^{58}Ni reaction using the ab initio density distribution*, European Physial Journal A, 48, 145.